The fracture behaviour of a PXE/HIPS polyblend

C. M. Rimnac, R. W. Hertzberg and J. A. Manson
Materials Research Center, Lehigh University, Bethlehem PA 18015, USA
(*Received* 20 *November* 1981; *revised* 16 *March* 1982)

As part of an overall examination of the fatigue crack propagation (FCP) behaviour of impact-modified polymers, a study of the fracture morphology of a PXE/HIPS polyblend polymer subjected to monotonic and cyclic loading conditions is reported. The HIPS rubbery-phase particles are found to fail by particle rupture in both fatigue and fast fracture. Another impact modifying addition, PE, is found to fail by a combination of interfacial rupture and tearing, the balance depending on the prevailing stress intensity value and the strain rate. Matrix failure is *via* multiple crazing at low fatigue crack growth rates, but shear yielding is believed to become a major fracture mechanism with increasing ΔK. The degree of plastic deformation of the matrix increases with increasing strain rate. This fact is manifested by the increasing void size associated with the interfacial separation of the PE particles.

Keywords Polyblend; poly(xylenol ether) blend; fracture; fatigue; crazing; shear

INTRODUCTION

As sophistication in polymer processing has increased, the toughening of brittle polymers by the mechanical blending or chemical grafting of an elastomer or rubbery component into the matrix has received increasing attention[1-10]. In particular, there has been interest in identifying the mechanisms by which these additions toughen the matrix. The generation of short, localized crazes and shear banding are believed to be mainly responsible for the observed toughening and to lead to an increase in the energy required for fracture[6].

Consistent with this observation, the addition of a rubbery second phase has also been found to improve the fatigue crack propagation (FCP) resistance of several polymers[11-14]. For example, plots of the fatigue crack growth rate, da/dN, vs. stress intensity level, ΔK, are shown for two polymers (polystyrene and poly(vinyl chloride)) in the neat and rubber-modified condition in *Figure 1*. Also shown are FCP data for poly(xylenol ether) (PXE) modified with high impact polystyrene (HIPS). (Polymer blends of this type are known commercially as Noryl.) It is clear that the FCP resistance of these polymers is improved through the addition of a rubbery component.

The investigation of a fracture surface generated during cyclic loading can be enlightening as to those fracture mechanisms responsible for the material's failure. For polymeric materials, two common fractographic markings can be present: discontinuous growth (DG) bands and fatigue striations[15-17]. Both markings appear as lines or bands lying perpendicular to the direction of crack growth.

Discontinuous growth bands are the result of the formation of one or at most a few crazes at the crack tip. The principal craze develops and gradually breaks down over several hundred to thousands of loading cycles. When the craze fibrils are sufficiently weakened, the crack front advances by striking through the craze zone. The width of a DG band has been found to vary with the square of ΔK; therefore, the width increases with increasing crack length.

Fatigue striations correspond to the advance of the crack tip during each loading cycle. The spacing between these lines is a record of the increment of crack growth per cycle and, as such, can be compared with the macroscopic fatigue crack growth rate, da/dN, when striation formation takes place. An excellent one-to-one correspondence between the microscopic striation spacing and the macroscopic fatigue crack growth rate has been found for several polymeric materials[16].

A report is presented on an investigation of the fatigue fracture surface micromorphology of PXE/HIPS blends and how it compares to surfaces produced during fast fracture. To our knowledge, little work has been reported on the morphology of PXE/HIPS blends fractured under cyclic loading conditions, although the fast-fracture morphology of related polymer systems has been documented[6,7].

EXPERIMENTAL

Sheets (6.4 mm thick) of poly(xylenol ether) (formerly described as poly(phenylene oxide)) modified with high-impact polystyrene were obtained from the Westlake Plastics Company, Lenni, Pa., USA. As stated earlier, polymer blends of the type are known commercially as Noryl; the PXE/HIPS material used is the standard 'house blend', *circa* 1972.

Fatigue tests were conducted in the usual manner using compact tension specimens. Several Izod specimens were also tested, as well as a pre-notched specimen broken in 4-point bending at a slow (but undetermined) rate. In addition, one tensile test was performed at a crosshead speed of 0.08 mm/s.

Fractographic analysis was conducted on an ETEC scanning electron microscope (SEM) at an accelerating voltage of 20 kv. The specimens were sputter coated with a gold-palladium alloy prior to examination.

0032-3861/82/131977 06$03.00

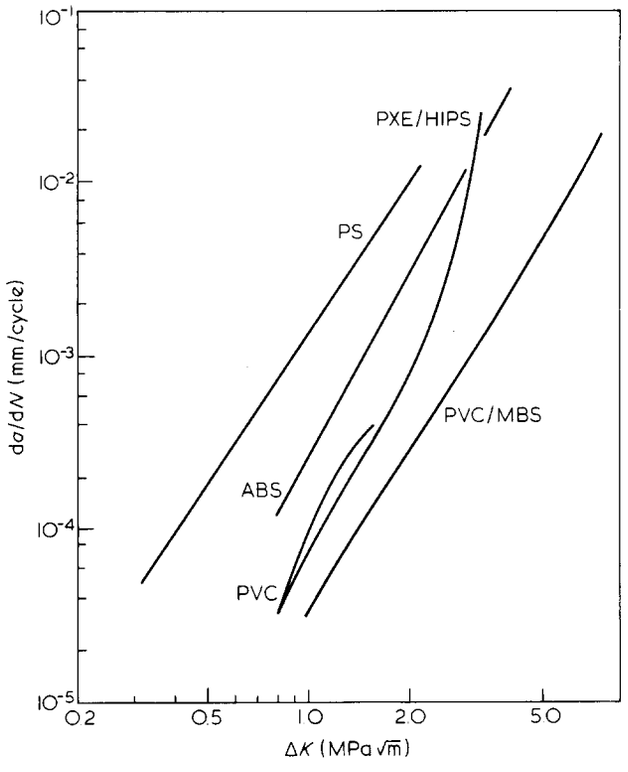

Figure 1 Plot of fatigue crack growth rate, da/dN, vs. stress intensity level ΔK for PXE/HIPS polyblend and for PS and PVC in the neat and rubber-modified condition, 10 Hz

MATERIAL CHARACTERIZATION

The PXE/HIPS polyblend is typically a 60:40 (by weight) blend of PXE and HIPS, the latter being a blend of polystyrene (PS) and polybutadiene (PB). In addition, polyethylene (PE) beads are said to act as an aid to processing and as an inexpensive filler[18]. In order to examine the nature and size of the modifying additions, sections of the polyblend were exposed to gaseous OsO_4 for one week and then ultramicrotomed into thin films for viewing by transmission electron microscopy (*TEM*). *Figure 2* is a transmission micrograph of a thin film revealing the typical structure of a rubbery particle derived from the HIPS. The dark continuous material (A) is the polybutadiene phase which has been attacked by the OsO_4. The clear, discontinuous occluded particles (B) are polystyrene and the matrix between the dual-phase particles is the miscible blend of PS with PXE (C). Measurements of the rubbery particles show that they range in size from 1 to 10 μm, with the majority having a diameter of about 5 μm.

Since PE is a saturated polymer, it is not stained by OsO_4 and hence is not revealed in thin films like the one shown in *Figure 2*. An alternative method was then required to identify the PE particles and follow their behaviour in the polymer blend. By separating the PE the matrix *via* dissolution of the matrix followed by filtration, identification of the PE beads was achieved using differential scanning calorimetry (d.s.c.). The melting temperature (T_m) of the filtered PE was compared to typical PE's and found to be in good agreement (T_m of filtered unknown = 101°C, T_m of PE film = 106°C, and T_m of bulk PE = 91 C). As discussed below, the PE particles were found to be spherical in shape with a diameter of approximately 1 μm.

FRACTURE SURFACE MICROMORPHOLOGY

The effectiveness of a rubbery addition in improving the FCP resistance of a polymer is a complex function of the additive's concentration, shape, size and distribution. Furthermore, the nature of the particle–matrix interface is also an important consideration. For the case of PXE/HIPS polyblends, the response to cyclic and monotonic loading of the matrix, and of both the rubbery and PE phases can be examined in the scanning electron microscope (SEM). As will be shown, the rubbery particles failed by particle fracture, whereas the PE exhibited in some instances a high degree of interfacial debonding and in other cases considerable drawing and eventual tearing.

Fracture surface micromorphology-cyclic loading

Let us consider first the fracture behaviour of the duplex-phase rubbery particles during cyclic loading at low crack growth rates ($< 7 \times 10^{-4}$ mm/cycle). Since there is strong interfacial bonding between the rubbery phase and the PS component of the HIPS and good miscibility of the PS with PXE (presumably resulting in a strong entanglement network), failure of these particles occurs by internal rupture, rather than by interfacial decohesion. For example, a ruptured rubbery particle is shown in *Figure 3* with the occluded spherical regions being the internal PS phase (recall *Figure 2*); the polybutadiene phase that surrounds the PS spheres is drawn out before final rupture. Note also the relatively continuous interfacial bond which apparently exists between the rubbery particles and the matrix. A similar fracture surface micromorphology was reported earlier by two of the authors for a simple HIPS polymer[14]. At higher crack growth rates ($> 10^{-3}$ mm/cycle), the fracture surface exhibited parabolic markings, with the parabolae opening up in the direction of crack growth (*Figure 4*). A similar appearance has been observed on the fast fracture surfaces of several polymers and is believed to be due to impurities or particles fracturing ahead of the main crack front[19,20]. In the PXE/HIPS polyblend, the initiation of these fracture parabolae is traced to the rupture of the rubbery particles from the HIPS component (note arrows in *Figure 4*).

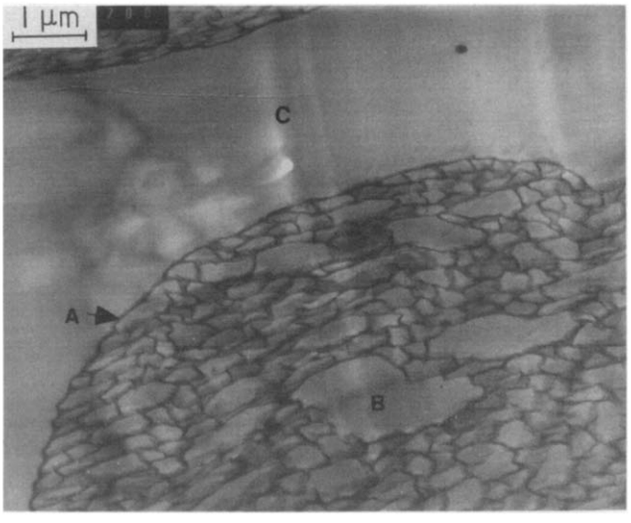

Figure 2 OsO_4 stained *TEM* of PXE/HIPS thin film. (a) Stained PB, (B) occluded PS, (C) matrix/rubbery phase interface

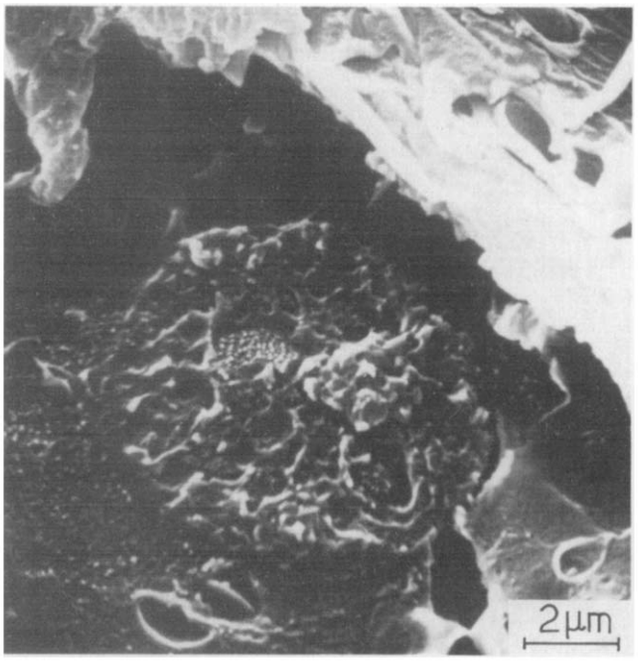

Figure 3 High magnification view of fractured HIPS particle. (ΔK = 1.2 MPa $\sqrt{m}$)

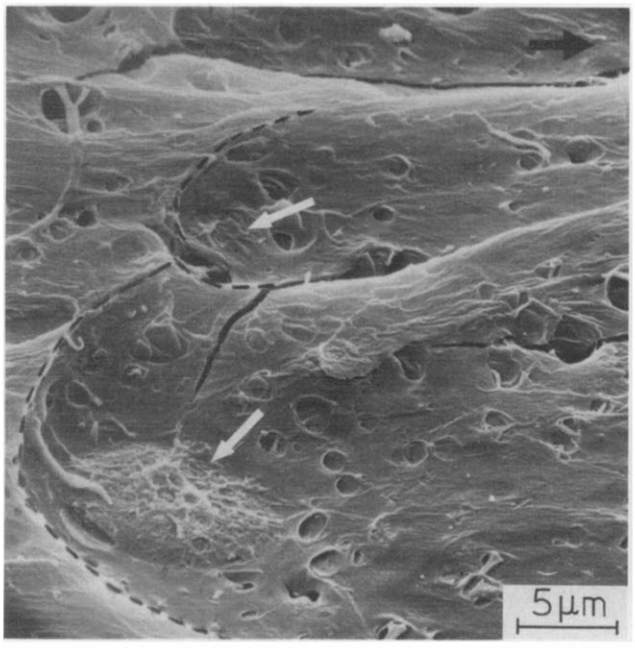

Figure 4 Fatigue fracture surface of PXE/HIPS polyblend at high ΔK showing the appearance of parabolae, with HIPS particles at their focii. Black arrow indicates direction of crack growth (ΔK = 3.4 MPa $\sqrt{m}$)

In contrast to the rubbery particles, the PE particles exhibited predominantly interfacial failure at low fatigue crack growth rates ($<5\times10^{-5}$ mm/cycle). Several of these spheres are seen in *Figure 5a* (X) along with some depressions in the matrix (Y); the latter surely represent sites where PE beads had been pulled out and presumably remained attached to the mating fracture surface. Measurements of the sizes of these holes as well as the matrix areas surrounding the embedded PE beads are consistent with the size of the PE beads. From this, we conclude that the matrix experienced little overall plastic deformation under the small-strain-high cycle conditions associated with low FCP rates. Instead, the small-strain-amplitude cyclic conditions contributed to a breakdown of the intrinsically weak PE-matrix interface prior to significant deformation of the PE particles. It is interesting to note that very low FCP rates in metal alloys also lead to interfacial breakdown between inclusions and the alloy matrix. Some limited plastic deformation did occur in the PE particles as evidenced by their slightly elongated shape (*Figure 5b*). In addition, a number of PE particles revealed evidence of localized tearing; note the shard of material torn away from the PE bead at A. In fact, there is strong evidence to suggest that the PE beads are

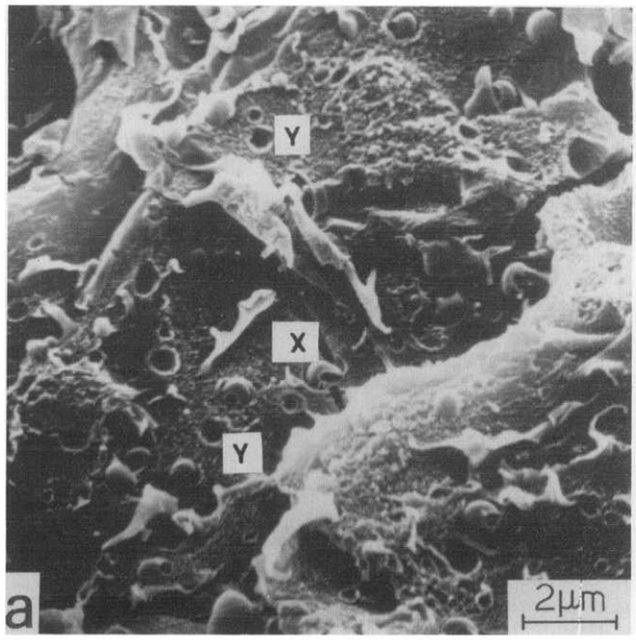

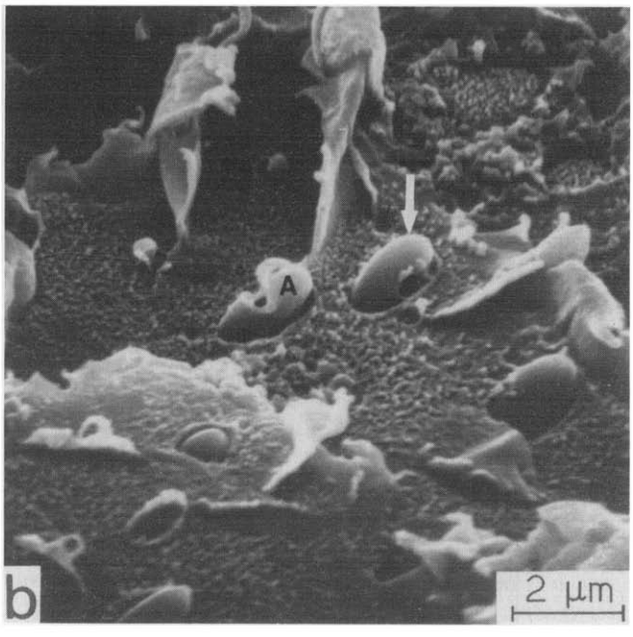

Figure 5 (a) Fatigue fracture surface of PXE/HIPS polyblend at low ΔK showing slightly elongated PE particles (X) and associated depressions in the matrix (Y). (b) Higher magnification view of PE particles revealing localized tearing (A). (ΔK = 0.9 MPa $\sqrt{m}$)

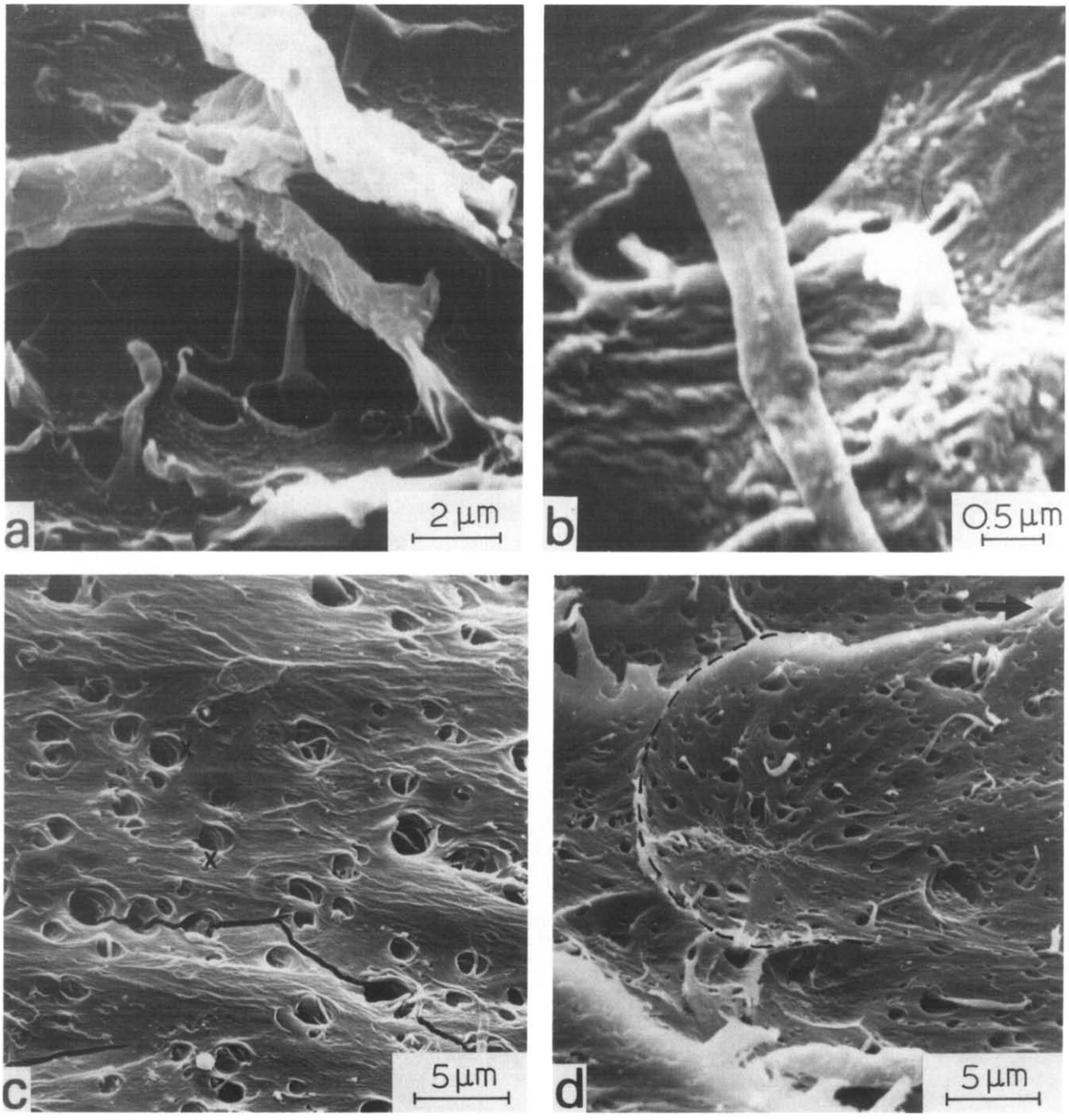

Figure 6 (a) Drawn PE particles at high ΔK (~3 MPa $\sqrt{m}$). (b) Higher magnification view of highly drawn PE particle. (c) Fatigue fracture surface of PXE/HIPS polyblend at high ΔK revealing drawn PE, matrix voids containing PE remnants (X) and secondary cracking. (d) Slow tearing initiation zone of slow bend specimen revealing highly drawn PE

hollow and tend to tear open near those localized regions where the balloon-like beads are attached to the matrix phase.

With increasing crack growth rates, the hollow PE beads experienced progressively greater amounts of tearing to the point where they appeared as highly drawn strands of material (*Figure 6a, b*). In such instances, it is believed that the PE particles were attached to the matrix only in two widely isolated areas. Apparently, at the larger strain-amplitude conditions associated with the higher FCP rates, the PE particles became extended and finally tore apart before the PE-matrix interface broke down. Measurement of the diameters of the matrix holes to which these PE shards are attached revealed their diameters to be roughly twice that of the undeformed PE bead. Thus, both the matrix and PE phases underwent considerably more plastic flow when the cyclic strains associated with higher crack growth rates were imposed. In this crack growth regime, there were also many voids on the fracture surface which appeared to contain a concentric ring of material (X) below the plane of intersection between the void and the overall fracture plane (*Figure 6c*). It is suggested that if the PE particle had adhered to the matrix in several widely spaced locations, then failure of the hollow bead would involve tearing along its equatorial plane; the fractured PE hemisphere would then be expected to relax back into the void and appear as a circular ring on the void walls.

The behaviour of the matrix during fatigue loading is also of interest. At low crack growth rates, the matrix has a rough, stippled appearance, reflecting the path of the crack through a craze (*Figure 5b*)[14]. In addition, the crack tended to progress along several parallel planes (*Figure 5a*). It is likely that at this low stress intensity level failure took place after the development of multiple crazes. At higher crack growth rates, the matrix appeared smoother in texture and drawn in the direction of crack growth (*Figure 6c*). This morphology reflects a much greater level of plastic flow of the matrix (which was also indicated by the larger voids surrounding the PE particles). A similar finding was reported by Maxwell and Yee[6]. Thus, shear yielding is now believed to be the dominant mechanism of failure, although there is still evidence of some secondary crazing and associated cracking normal to the major plane of fracture (*Figures 4* and *6c*). The secondary crazes appeared to seek out the duplex-phase and PE particles which apparently acted as both sites for craze initiation and termination. On the other hand, Bucknall concluded that in PXE/HIPS blends subjected to monotonic tensile loading, crazes initiated at the duplex-phase particles, but then terminated mainly at shear bands[8].

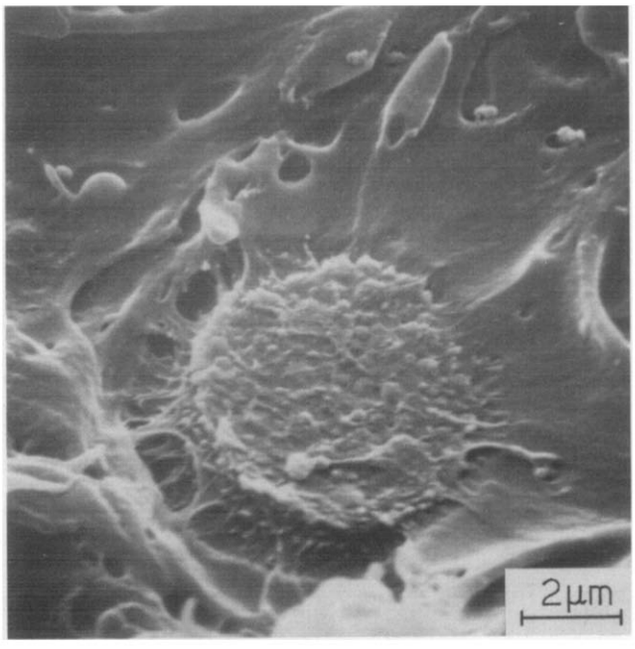

Figure 7 Rubbery particle (from HIPS component) ruptured during fast fracture showing extensive interfacial breakdown

Finally, superimposed on the micromorphology of the fatigue fracture surface just prior to the onset of fast fracture are bands which lie perpendicular to the direction of crack growth. In addition, the width of the bands increases with increasing stress intensity level. Measurement of their width reveal their size to be in agreement with the fatigue crack growth rate, da/dN. Therefore, these bands are classic fatigue striations, representing the successive position of the advancing crack front during each load excursion, as described earlier. No evidence to suggest the presence of discontinuous crack growth bands was found at any location on the fatigue fracture surface.

Fracture surface micromorphology-monotonic loading

At this point it is interesting to compare the fracture surface micromorphology of the unstable fracture zone in the fatigue samples with markings found in the stable fatigue zone (as described above). The duplex-phase particles were found to fracture again by internal rupture, though a greater degree of interfacial breakdown was noted than that observed under cyclic loading conditions (*Figure 7*). Also, the polybutadiene within a rubbery particle from the HIPS is not as highly deformed as was the case during fatigue. This is probably due to the much higher strain rate experienced in fast fracture, resulting in a smaller breaking strain of the particle.

Under the high strain rate, monotonic loading conditions associated with fast fracture, the PE particles were observed to separate at the interface from the matrix, somewhat like that noted earlier under low FCP rate conditions (*Figures 8a, b*). For this high strain rate condition, we speculate that the PE particles and the ligaments connecting the particles to the matrix suffer from a marked reduction in ductility. In analagous fashion, Sandiford and Willbourn showed that the total tensile elongation of low-density polyethylene decreases by an

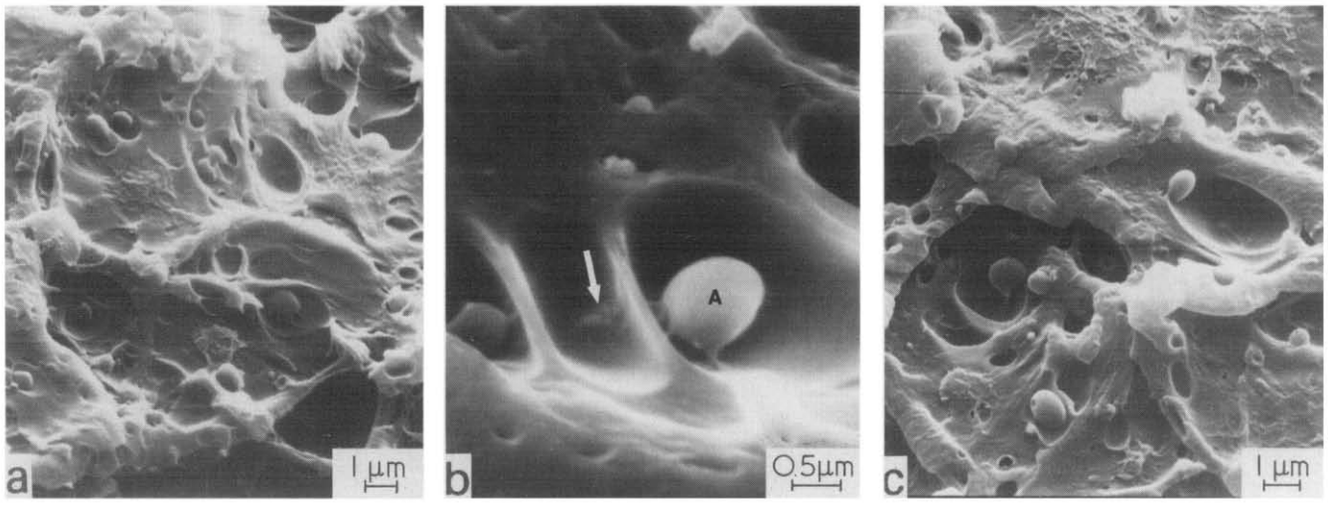

Figure 8 (a) Fast fracture appearance of fatigue specimen of PXE/HIPS polyblend. (b) Increased magnification showing essentially undeformed PE particle attached to PPO matrix at localized sites (A). (c) Fast fracture appearance of tensile strip of PXE/HIPS polyblend

order of magnitude when the test temperature is reduced from 0°C to −25°C[21]. As a result, the PE particles remain essentially undeformed whereas the matrix deforms to a greater extent. In this instance, the voids were nearly three times larger in diameter than the spherical PE particles themselves. Apparently, the matrix underwent considerably more plastic flow during fast fracture at high stress intensity levels than that which occurred at much lower ΔK levels during fatigue crack growth (recall *Figure 5*)[6].

The fracture surface micromorphology shown in *Figure 8a* was noted also on fracture surfaces generated from Izod impact specimens, a tensile strip, and the unstable fracture zone from a pre-notched slow bend specimen (*Figure 8c*). Maxwell and Yee have observed a similar fracture morphology in poly(carbonate)–poly(ethylene) blends tested under tensile loading conditions[6].

The slow bend specimen broken in this study also contained a region of slow tearing adjacent to the machined notch root. The fracture surface of this zone contained PE particles which were heavily drawn (*Figure 6d*) as was the case for intermediate and high fatigue crack propagation rates (recall *Figures 6a–c*). Therefore, cold drawing of the PE particles took place in connection with low strain rates and high plastic strains under both cyclic and monotonic loading conditions.

Returning to *Figure 8b*, it is interesting to note that the PE particle at A is attached to the matrix in only isolated regions. This confirms our earlier hypothesis that the bond between the PXE matrix and the PE particle is restricted to localized sites. Also, at the base of the void in the centre of the photograph, there are several small nubs, possibly remnants of the PE particle which once created the void. The majority of this particle is likely to be found on the mating fracture surface with part of its balloon-like skin torn away, as observed at low fatigue crack growth rates (recall *Figure 5b*).

CONCLUSIONS

The fracture surface micromorphology of the PXE/HIPS polyblend (containing a PXE/PS matrix and two toughening phases, PE and a composite PB/PS particle from the HIPS) has been characterized under cyclic and monotonic loading conditions. The PB/PS particles fail by particle fracture, during both fatigue and fast fracture, while the PE particles can fail interfacially and plastically deform, depending on the stress intensity level and strain rate. At very low fatigue crack growth rates, the PE particles deform little and failure is interfacial. At high fatigue crack growth rates, the PE particles are either highly elongated, or the particle fractures and the failed hemisphere relaxes into its matrix void. During fast fracture, the strain rate is high and the PE particles remain essentially undeformed, with failure taking place at the particle–matrix interface.

Finally, the matrix fails by multiple crazing at low stress intensity levels, but with increasing ΔK levels, shear yielding predominates. Plastic deformation of the matrix increases with increasing strain rate, as witnessed in the increasing size of the voids associated with the PE particles, from low crack growth rates through to fast fracture.

ACKNOWLEDGEMENTS

The authors gratefully acknowledge the support provided by IBM and the Polymers Program of the National Science Foundation (Grant No. DMR-8106489). They also appreciate the assistance of Sally M. Webler in determining the melting temperatures of the PE component of the polyblend.

REFERENCES

1 **Bucknall, C. B. and Clayton, D.** *J. Mater. Sci.* 1972, **7**, 202
2 **Bucknall, C. B., Clayton, D. and Keast, W. E.** *J. Mater. Sci.* 1972, **7**, 1443
3 **Bucknall, C. B. and Drinkwater, I. C.** *J. Mater. Sci.* 1973, **8**, 1800
4 **Bucknall, C. B. and Stevens, W. W.** *J. Mater. Sci.* 1980, **15**, 2950
5 **Petrich, R. P.** *Polym. Eng. Sci.* 1973, **13**, 248
6 **Maxwell, M. A. and Yee, A. F.** *Polym. Eng. Sci.* 1981, **21**, 205
7 **Yee, A. F.** *J. Mater. Sci.* 1977, **12**, 757
8 Bucknall, C. B., 'Toughened Plastics', Applied Science Publishers, London, 1977
9 Manson, J. A. and Sperling, L. H., 'Polymer Blends and Composites', Plenum Press, New York, 1976
10 Yee, A. F., Olzewski, W. V. and Miller, S., 'Toughness and Brittleness of Plastics', (*ACS Adv. Chem. Series*), 1976, **154**, p. 97
11 Skibo, M. D., Janiszewski, J., Hertzberg, R. W. and Manson, J. A. 'Toughening of Plastics', Plastics Rubber Institute, London, July, 1978, Paper No. 25
12 Skibo, M. D., Manson, J. A., Webler, S. M., Hertzberg, R. W. and Collins, E. A. *ACS Symposium Series No. 95*, (Ed. R. K. Eby), 1979, 44077
13 Hertzberg, R. W., Skibo, M. D. and Manson, J. A. *ASTM STP 700* 1980, 49
14 Manson, J. A. and Hertzberg, R. W. *J. Polym. Sci. Polym. Phys. Edn.* 1973, **11**, 2483
15 Manson, J. A. and Hertzberg, R. W. *CRC Crit. Rev. Macromol. Sci.* 1973, **1**, 433
16 Hertzberg, R. W., Skibo, M. D. and Manson, J. A. *ASTM STP 675* 1978, 471
17 Skibo, M. D., Hertzberg, R. W., Manson, J. A. and Kim, S. L. *J. Mater. Sci.* 1977, **12**, 531
18 Gowan, C. A. US Pat. 3361851, Jan. 2, 1968
19 Hull, D. 'Polymeric Materials', ASTM, 1975, p 526
20 Haward, R. N. Ed., 'Physics of Glassy Polymers', Halsted Press, New York, 1973, pp 388–390
21 Ritchie, P. D. Ed., 'Physics of Plastics', D. Van Nostrand Co. Inc., Princeton, NJ, 1965, p 43